# Multifunction Imaging Passive Radar for Harbour Protection and Navigation Safety

**Amerigo Capria[(1)], Elisa Giusti[(1)], Christian Moscardini[(1)], Michele Conti[(1)], Marco Martorella[(1)(2)], Dario Petri[(1)], Fabrizio Berizzi[(1)(2)]**

**(1) RaSS National Laboratory, CNIT (National Inter-University Consortium for Telecommunications), Pisa, Italy**

**(2) Department of Information Enginering, University of Pisa, Italy**

## ABSTRACT

In this work, the capabilities of Passive Bistatic Radars (PBRs) for monitoring marine traffic and, more in general, for situation awareness in the proximity of a harbor have been addressed. Capabilities such as detection, tracking and possibily Inverse Synthetic Aperture Radar (ISAR) imaging have been demonstrated for maritime targets. The Livorno harbour has been considered as a specific case study as it is a relatively busy maritime hub. The experimental results have clearly shown that PBRs represent a viable solution for monitoring maritime traffic and to provide information for a common operational picture in harbour areas.

## INTRODUCTION

In maritime domain awareness scenario, two main areas of interest can be recognized, specifically harbour protection and navigation safety. Harbour protection is currently a main concern and it is aimed at controlling the risk associated with possible attacks or illegal activities which can take place in the marine access areas. On the other hand, the objectives of the navigation safety are essentially connected to achieve an improved maritime navigational awareness through collision avoidance information and guidance advices to the navigators [1].

Nowadays, maritime traffic control is performed via the VTS (Vessel Traffic Service) system, which usually exploits the information provided by the AIS (Automatic Identification System) installed on board of cooperative vessels. Such system allows for port authorities to know the GPS position of vessel equipped with a functioning AIS device, thus providing the means for controlling and monitoring an area of interest. Maritime traffic control systems are usually equipped with a ground segment, which consists of a coastal surveillance radar, which is able to detect all vessels, both cooperative and non-cooperative, and to provide an "all-weather" and "all-day" monitoring of a large area of interest.

However, because of the continuous increase of the maritime traffic, modern maritime traffic control systems are demanded to strengthen the harbor protection and navigation safety level without greatly affecting the e.m. pollution level. Moreover, it is not always feasible for port authorities to invest in an expensive infrastructure of primary radars. Therefore, cost-competitive passive radars exploiting illuminators of opportunity may provide a better means to manage vessel traffic within a harbor. This can include monitoring of potentially malevolent operators, such as illegal fishing vessels, hazardous cargo transporters and smugglers.

Passive Bistatic Radars (PBR) have gained a lot a attention in the last few years from the scientific community [2]-[15] because of several reasons, among all, the possibility to exploit digital IOs with relatively large bandwidth and high transmitted power and the availability on the market of low cost high speed digital acquisition systems. Moreover, as research in this field has progressed, new radar techniques have improved PBRs to the point to make them able to handle several tasks and to be effectively deployed in several scenarios. Examples of such tasks are array processing for target DoA estimation and radar imaging of moving targets. Obviously, there are some drawbacks in operating with a PBR, among all, the fact that both the transmitted waveform and the transmitted power are not under the control of the radar designer. However, to better

handle these issues, research in this field has also progressed with the development of multiband passive radar that can operate with different IOs.

The primary objective of this work is to demonstrate the effectiveness of using passive radars with imaging capability for monitoring marine traffic and for improving the situational awareness in the proximity of a harbor. In details, a PBR can offer radar detection and tracking functionalities for navigation safety purposes and simultaneously provide radar imaging capability.

The PBR demonstrator used for the purpose of this work is named SMARP (Software-defined Multiband Array Passive Radar) and it has been conceived in the framework of the Italian National Plan for Military Research by the Radar and Surveillance Systems Laboratory (RaSS Lab.) of the Italian National Inter-university Consortium for Telecommunications (CNIT). The SMARP demonstrator peculiar features are listed here:

- Multiband receiving array antenna (UHF and S band) with dual polarization reception;
- Software-defined multiband flexible receiver based on commercially available solutions;
- Digital array processing techniques and advanced radar signal processing algorithms implemented on COTS (Commercial Of The Shelf) processing architectures (multicore CPUs and GPUs);

Such features allow for a great flexibility such as the use of both DVB-T and UMTS IOs for detection and tracking of targets in the range-Doppler map. Moreover, the use of array processing allows for the estimation of the target DoA thus allowing for accurate target localisation. Radar imaging functionality is instead activated on demand by using a wider bandwidth signal. Signal with wide enough bandwidth may be obtained for example by coherently combining adjacent DVB-T or UMTS channels.

## SMARP SYSTEM DESCRIPTION

The SMARP system architecture [16] is reported in Figure 1. The main functional blocks are:

- The antenna system, namely, an array for the surveillance channel and a dedicated single element for the reference channel;
- The RF-Front-End #1 and the calibration network;
- The RF-Front-End #2 which include the synchronization signal generator;
- Digital Signal Processor (DSP), Control Unit (CU) and Graphical User Interface (GUI);

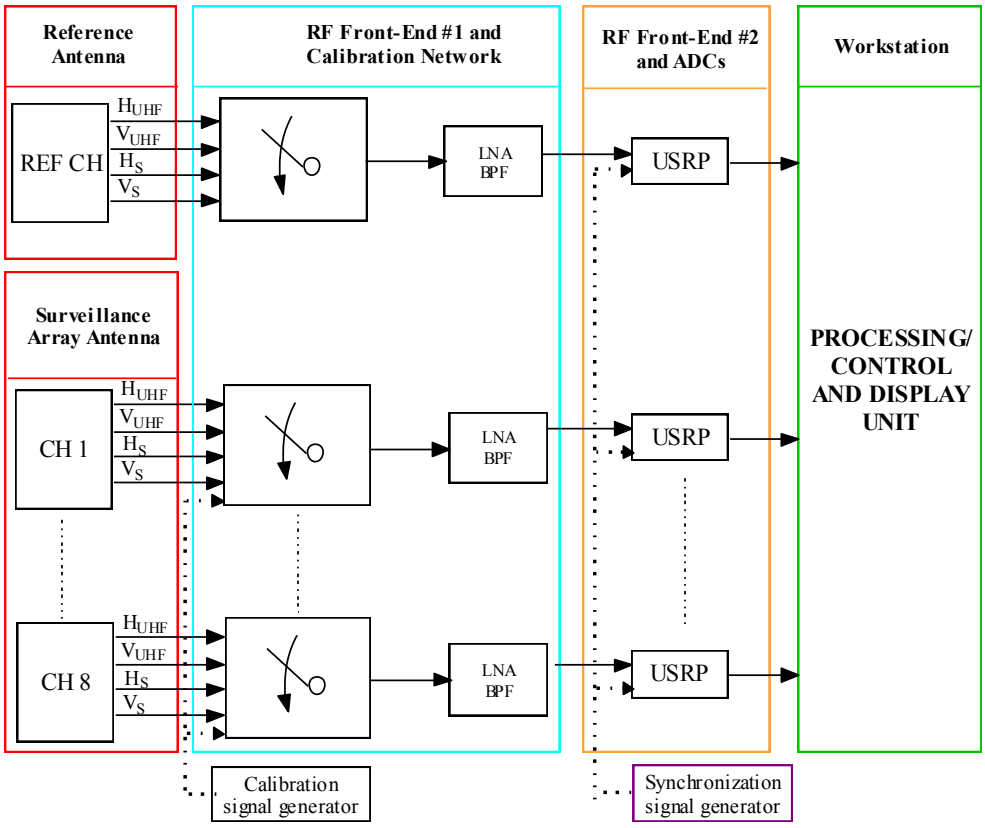


**Figure 1: SMARP system architecture**

Pictures of the SMARP system installed in Livorno are shown in Figure 2: where the main functional blocks have been circled with different colors.

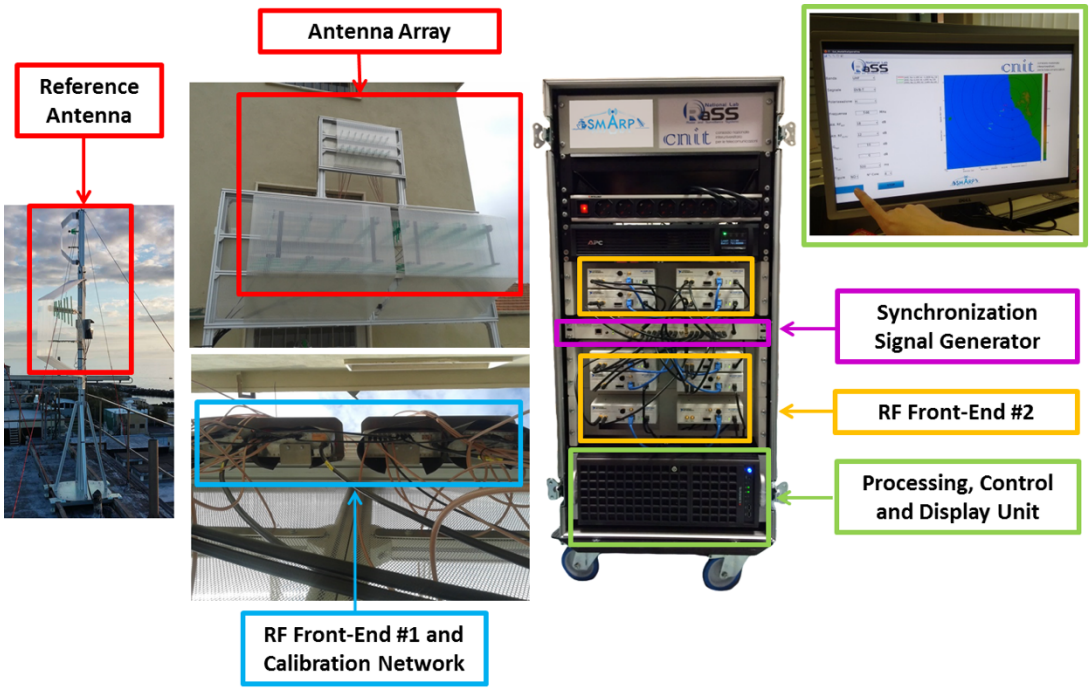


**Figure 2: SMARP subsystems**

### Antenna system

The receiving antenna is a dual band and dual polarization system. Its main features are:

- Multiband receiving array antenna: UHF-band (470-790 MHz) and S-band (2100-2200 MHz), with dual polarization reception (H/V)[17];
- Four linear arrays, two for each band, composed of 8 LPDA (Logarithmic Periodic Dipole Antenna) patch antennas. The inter-element spacing is equal to 30 cm in the UHF band and 8 cm in the S-band;
- The antenna is equipped with two plane reflectors, one for each band (UHF-band: 3.1x1.3x0.86m and S-band: 1.1x0.7x0.27m).

The reference antenna is composed of four separate receiving elements of the same type of the ones used for the surveillance antenna, one for each frequency band and polarization.

**RF Front-End #1 and Calibration Network**

The RF Front-End #1 contains the system input filters to reject the interferences out of the working frequency band, and the LNA to amplify the desired signal with a limiting effect on the system noise figure. A switch controls the selection of the total gain given by the amplification chain which is dependent on the signal exploited and on the e.m. environment.

The calibration routine estimates the constant phase offsets and amplitude imbalances, and generates the correction coefficients to be applied to the signal samples before digital beamforming. The selection between the calibration path and the antenna received signals path is performed by a switch which is remotely controlled via software. The signals coming from the antennas are the default inputs transferred to the RF-Front Ends #1. When the switches are set in "calibration mode", the RF-Front End #1 input changes to the calibration signal. During this phase, a board is used for generating and injecting, in a closed-loop mode, the calibration reference signal into the RF chains.

**RF Front-End #2**

The main receiver requirements to be satisfied for SMARP were identified by:

- Flexile reception in the bandwidth 470-790 MHz and 2100-2200 MHz;
- Receiving instantaneous bandwidth up to 7.61 MHz;
- Sampling resolution equal to 14 bits;
- Capability to operate in a coherent and synchronized multichannel configuration.

The selected solution for the SMARP receiver is based on a COTS Software Radio System from National Instruments, the NI USRP-2922. This board is a general purpose versatile transceiver able to fully meet the requirements. It can operate on a wide frequency band, specifically 400MHz -4.4GHz and it is equipped with an FPGA in charge of dealing with high data rate processing (e.g.: digital down conversion, decimation and so on).

**Synchronization Signal Generator**

To perform digital array processing, a synchronous and coherent multichannel acquisition system is mandatory. When operating with several USRPs boards, the mentioned requirements can be achieved by feeding each board with two reference signals, specifically:

- A 10MHz reference clock to provide a single frequency reference for all devices;
- A pulse-per-second (PPS) to enable a temporal synchronization of the acquired samples.

The generation of the reference signals has been achieved by using a clock distribution unit, produce by Ettus Research and named a OctoClock-G, which provides a suitable number of 10 MHz and 1PPS outputs (i.e.: equal to the number of NI USRP-2922 boards to be synchronized).

**Processing, Control and Display Unit**

The Digital Signal Processing (DSP) architecture is composed of the following blocks:

- Pre-processing to reduce the multipath effects and attenuate the spurious peaks caused by guard intervals, deterministic and pseudorandom pilot tones of the waveform [18].
- Range-Doppler (RD) map formation which aims at filtering out the direct path interference, its multipath and at generating the RD map for each receiving channel [19],[20],[21].
- Surveillance Channel Beamforming: this processing unit aims at forming one or more beams in the surveillance area. Moreover, this allows obtaining a raw estimation of the target DoA [22].
- Detection, which provides the target position in the RD domain. This step is accomplished by using Constant False Alarm Rate (CFAR) detection techniques.
- Tracker, which aims at reconstructing the path of targets in the RD domain [23].

- Graphical User Interface (GUI) which allows user to control the main system parameters (e.g. operating mode, frequency, integration time, amplification chain) and displays the radar output, namely the RD maps, results of detection and tracking on a georeferenced map.

## EXPERIMENTAL RESULTS

### Measurement Scenario

The SMARP demonstrator has been installed in Livorno on the roof of the CSSN-ITE "Istituto Vallauri". Different measurement campaigns have been carried out to perform detection of various vessels both arriving and departing from the Livorno harbour, by exploiting both DVB-T and UMTS signals. The surveillance antenna was directed towards an area of sea in front of the receiver site at an angular direction of about 260° as shown in Figure 3. A building which limits the visible area toward North is located at the direction of about 285°. The exploited transmitters of opportunity (see Figure 3) are respectively a DVB-T transmitter located on "Monte Serra" in Pisa (around 32 km far from the receiver) and a UMTS base station located at the stadium "Armando Picchi" (around 400 m far from the receiver). For this experiment the system has been configured to acquire wideband signals, up to 25 MHz. The used channels carrier frequencies were respectively 634 MHz and 2147.5 MHz. The wideband signal has been used for ISAR functionality, while detection and tracking functionality have been performed by using only one transmitted channel.

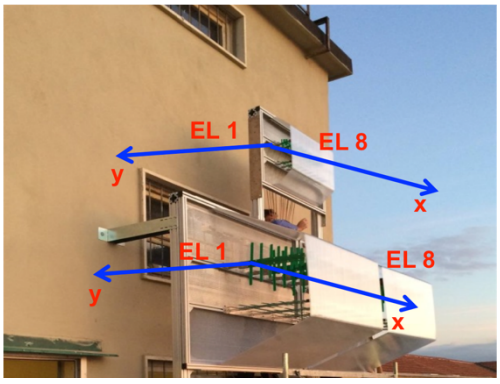


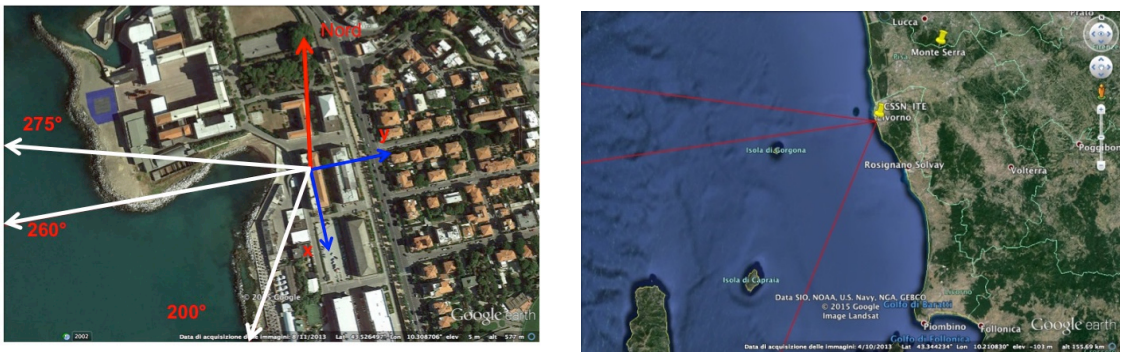


**Figure 3: Scenario Geometry**

## Detection and Tracking Capabilities

In this section, the preliminary results obtained during different measurement campaigns are presented. The actual trajectories of non-cooperative vessels have been recorded with an AIS (Automatic Identification System) receiver to be used for validating the detection and tracking functionalities of the system. The results are obtained by separately exploiting both bands of interest (i.e.: UHF and S-band). The integration time was 0.5s and the total duration of each acquisition was about 20 minutes. The main characteristics of the non-cooperative targets are shown in TABLE I.

TABLE I. TARGETS CHARACTERISTICS - UHF AND S BAND EXPERIMENTS

| Maritime Mobile Service Identity (MMSI) | Name | Type | Size | Exploited Bandwidth |
|---|---|---|---|---|
| 538090480 | Navin Vulture | Cargo | 113m x 17m | UHF |
| 248646000 | Loya | Tanker | 93m x 15m | UHF |
| 249830000 | Zim Luanda | Cargo | 260m x 32m | UHF |
| 247217500 | Grande Colonia | Cargo | 176m x 31m | UHF |
| 247131600 | Zeus Palace | Passenger | 212m x 25m | UHF |
| 304317000 | Anna Sophie Dede | Cargo | 135m x 23m | UHF |
| 470968000 | Al Bahia | Cargo | 306m x 40m | UHF |
| 247272700 | Elba | Tanker | 72.6m x 13.2m | S |
| 247000400 | Via Adriatico | Passenger | 150m x 23m | S |
| 247213700 | Fratelli Neri | Tug | 24m x 12m | S |

In Figure 4 and in Figure 5 the trajectories of the vessels acquired by the AIS receiver (coloured lines) are overlapped to the radar tracks (black lines). The estimated tracks well match the AIS trajectories thus confirming the effective operation of the SMARP demonstrator.

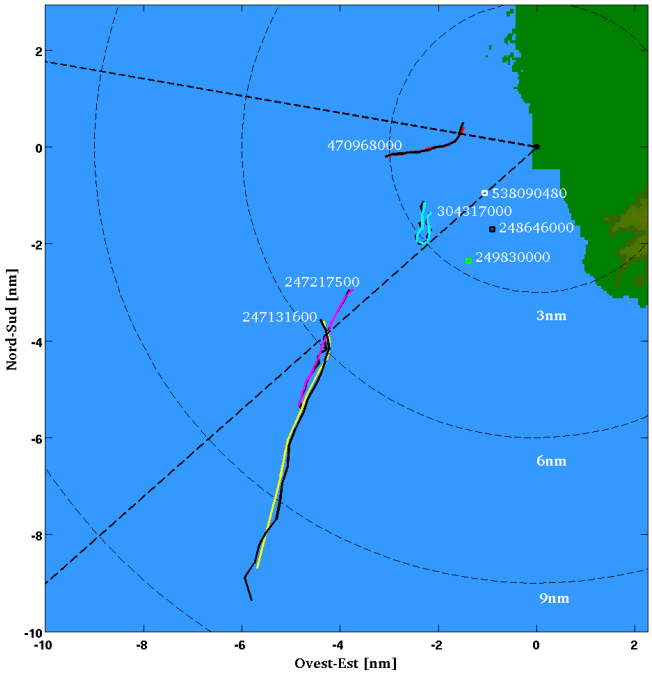


**Figure 4: AIS trajectories (coloured lines) and radar tracks (black lines) (UHF band)**

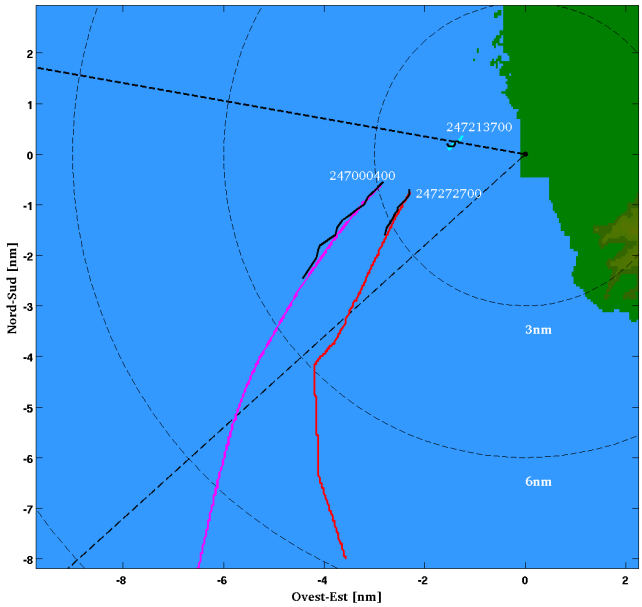


**Figure 5: AIS trajectories (colored lines) and radar tracks (black lines) (S band)**

The angular sector centred at the receiver site and plotted in Figure 4 and Figure 5 with a dotted black line is the HPBW of the single receiving element of the surveillance array, which exhibits a value of about 60°. Even though a number of detections were obtained well beyond this angular sector, it is expected to achieve reduced radar performance when operating outside the main beam of the surveillance antenna.

**ISAR Capability**

ISAR capability may be activated on a specific target of interest or may be performed simultaneously for all the detected targets. ISAR processing aims at providing well focused e.m. images of detected targets. ISAR images may provide additional information about the target, such as its size, shape and e.m. properties, which, in turn, may open the door to Automatic Target Classification or Automatic Target Recognition. The efficiency of ISAR images in providing useful information about the target depends, however, on the ISAR images quality and, in turn, on ISAR processing and the instantaneous transmitted bandwidth. Although the transmitted signal cannot be managed in a passive radar, recent works have demonstrated that an enhanced radar range resolution can be achieved by coherently adjoin adjacent DVB-T channels **Error! Reference source not found.**.

Nevertheless, it should be mentioned that the VHF/UHF spectrum is not completely filled with DVB-T transmissions, therefore leaving gaps in the frequency bandwidth. Such gaps produce grating lobes in the ISAR image when Fourier based ISAR imaging technique are used. For this purpose, an algorithm, based on Compressive Sensing (CS), able to extrapolate the missing signal in presence of frequency gaps, has been recently proposed [25].

In this experiments however, a signal composed of three adjacent DVB-T channels has been gathered, then the classical ISAR image processing which does not make use of CS, has been applied. Details about the Passive-ISAR imaging algorithm can be found in [26],[27].

After the detection and tracking steps, three targets have been chosen to show the results of the Passive-ISAR algorithm. Specifically, "Anna Sophie", "Grande Colonia" and "Al Bahia" vessels have been considered (dimensions shown in TABLE I. ).

All the targets underwent complex motion, either because they were manoeuvring and because of the sea state that during the experiments was moderate. Consequently, well focused ISAR images of the target can be obtained by processing portions of the data corresponding to an integration time smaller than the observation time. Figure 6, Figure 7 and Figure 8 show the ISAR images of the three considered targets. The observation time was 40 seconds, while the CPIs used to form the ISAR images are detailed in each figures. The estimated length of the targets are shown in TABLE II. Specifically, ISAR images on the left are shown in the Range/Doppler domain, which is the natural output of an ISAR processing. Conversely, ISAR images on the right are shown in a fully spatial coordinate system, namely Range/Cross-Range domain.

As can be noted by looking at Figure 6, the target changes its orientation in the Image Projection Plane (IPP) proving that the target is manoeuvring. Probably, only a side of the ship is imaged due to the low grazing angle under which the target is illuminated and observed. Because of the target's complex motions, the two-dimensional IPP orientation may change from frame to frame. Since the two-dimensional ISAR image is the result of a projection and convolution of the 3D target reflectivity function onto an unknown 2D plane, the target size could be underestimated and may change over time. This may lead to an incorrect estimation of the target geometrical features.

TABLE II. ESTIMATED LENGTH OF MEASURED TARGETS

| VESSEL NAME | FRAME# | ESTIMATED LENGTH | REAL LENGTH |
|---|---|---|---|
| Anna Sophie | 1 | 119 M | 135 M |
| Anna Sophie | 2 | 115 M | 135 M |
| Anna Sophie | 3 | 129 M | 135 M |
| Anna Sophie | 4 | 109 M | 135 M |
| Grande Colonia | 1 | 178 M | 176 M |
| Grande Colonia | 2 | 168 M | 176 M |

| | | | |
|---|---|---|---|
| Al Bahia | 11 | 287 м | 306 м |
| Al Bahia | 28 | 310 м | 306 м |

However, the use of a sequence of ISAR images instead of a single one, may partially overcome this issue and could provide a better estimate of the target length.

As an example, the overall estimated size of target "Anna-Sophie" results in 129 m, which is quite accurate.

**[dB]**

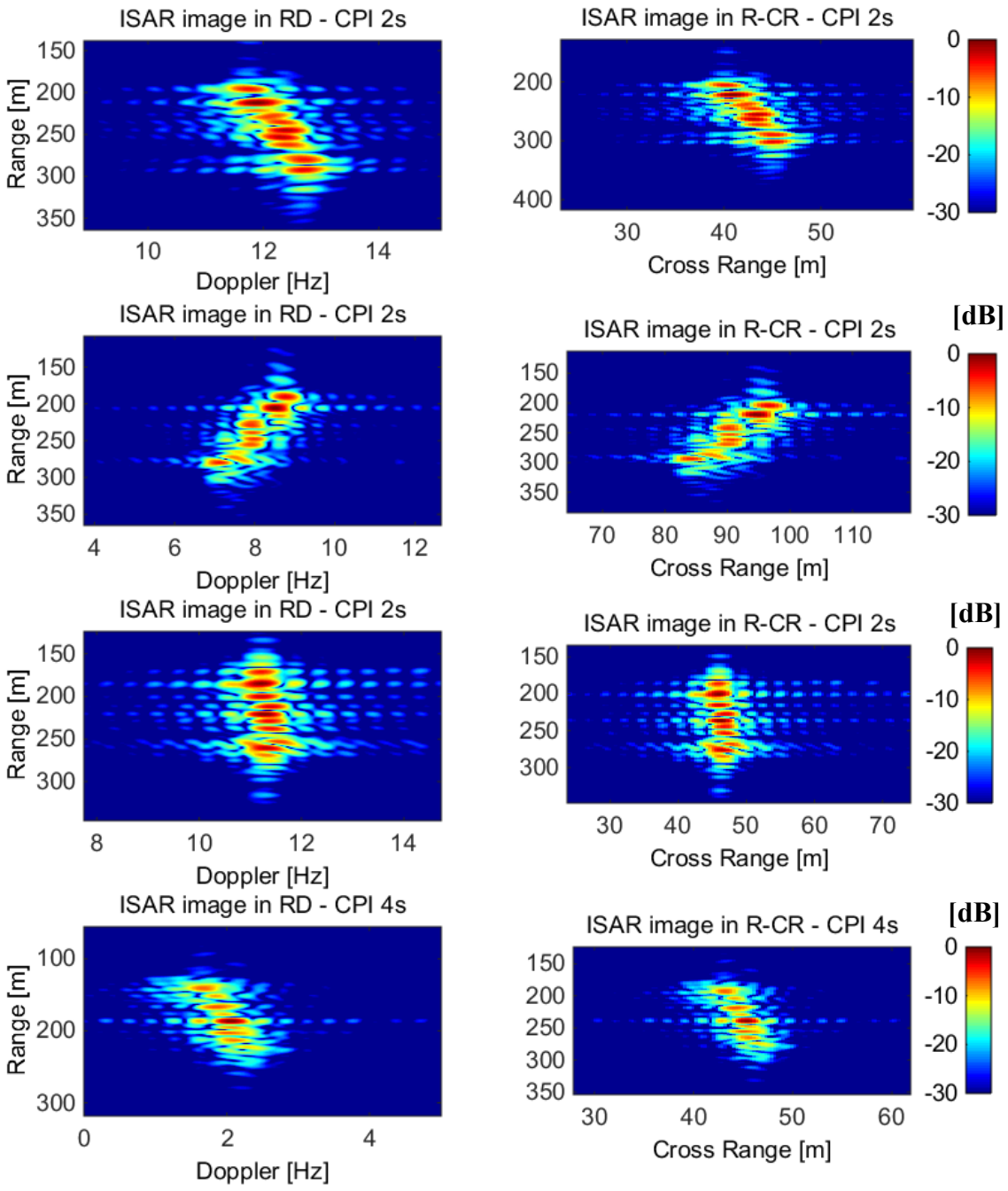


**Figure 6: ISAR images of "Anna Sophie" - UHF band**

Also for the "Grande Colonia" (Figure 7), target experiences complex motion as it changes its orientation in the IPP. The estimated size of such target is 178 m. Its true length is 176 m. Since the range resolution is 6.5 m, then the estimate is consistent with the target length.

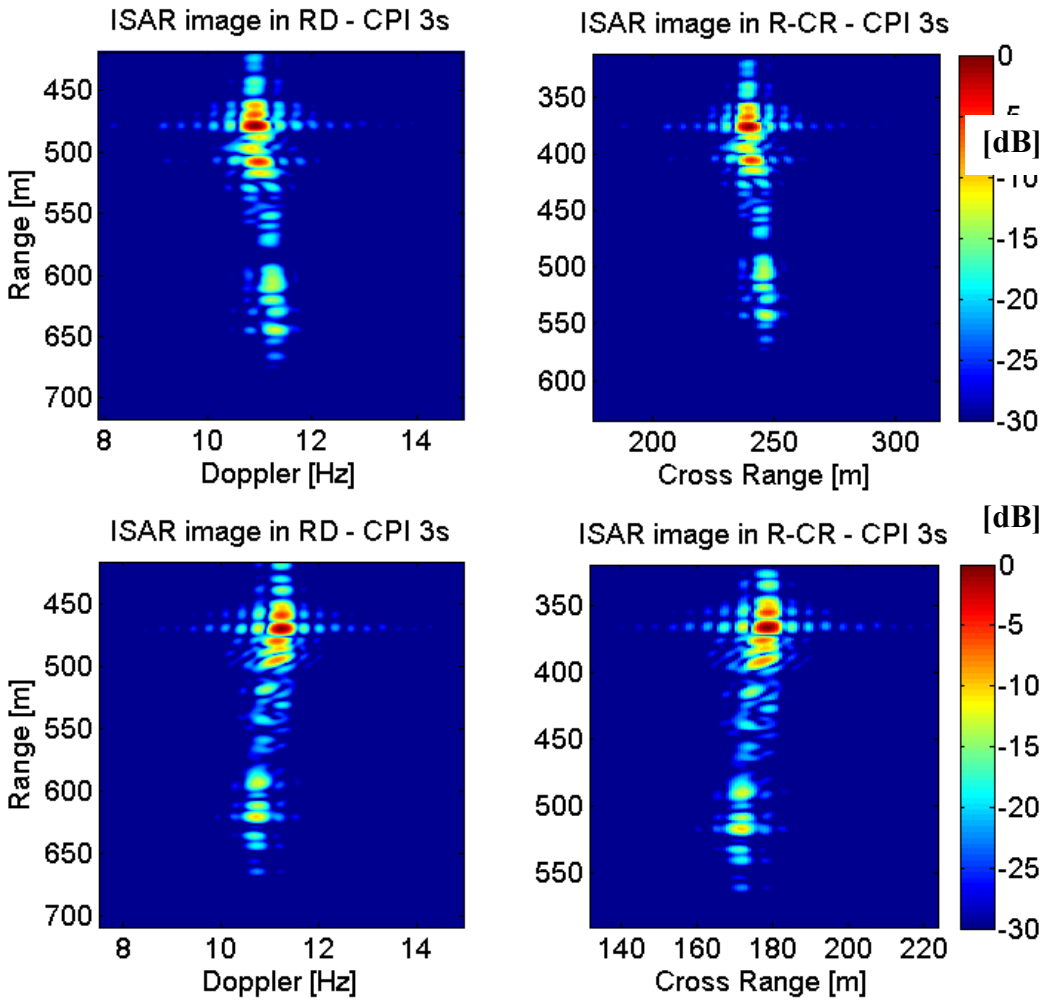


**Figure 7 : ISAR images of "Grande Colonia" - UHF band**

Regarding the third target (Figure 8) the estimated length from the ISAR images is 310 m while its actual length is 306 m.

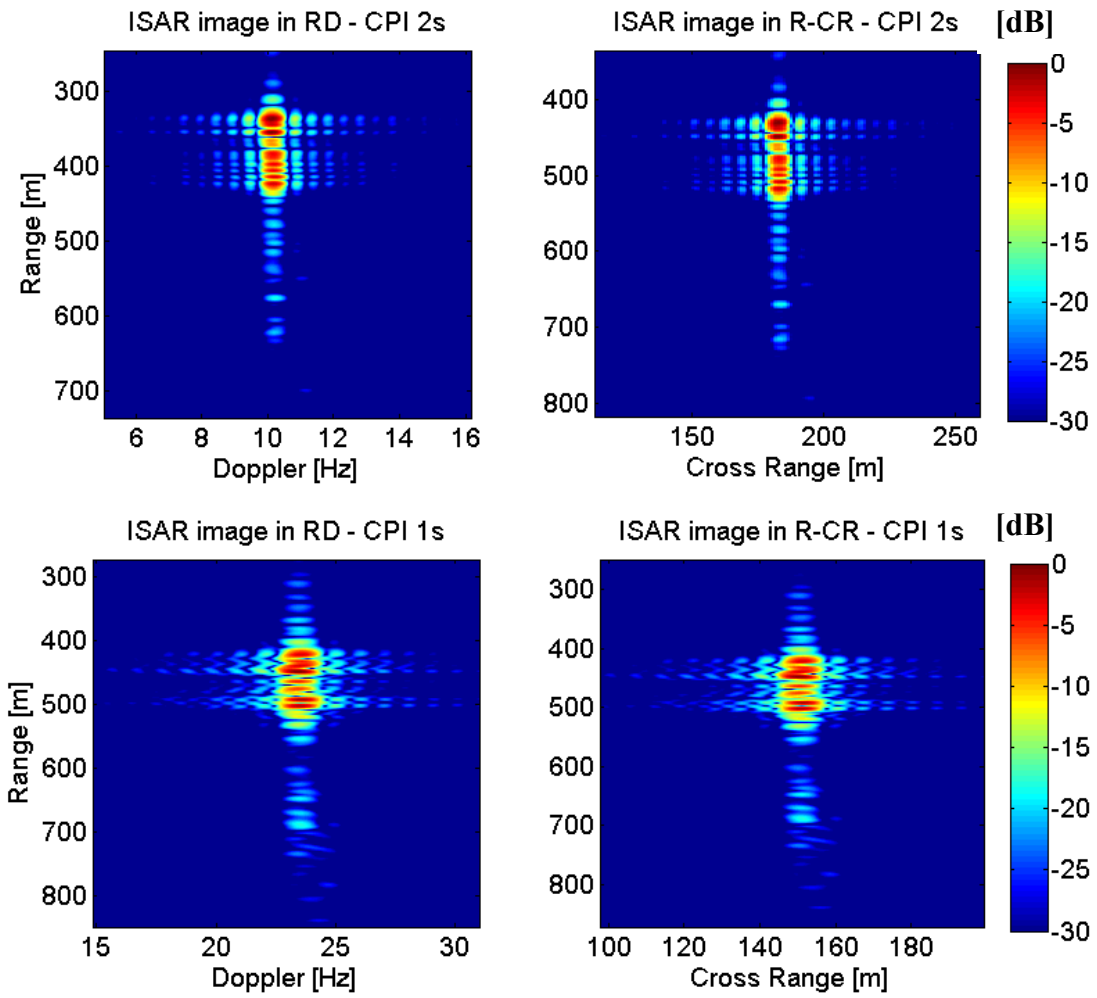


**Figure 8: ISAR images of "Al Bahia" - UHF band**

As can be noted from Figure 8, almost half of the target is shadowed. Shadowing effect is in this case probably due to low grazing angles of both transmitter and receiver, as well as the highest part of the ship which probably determines a shadowed area.

Despite of that, some scatterers of the stern are visible, even if with low RCS, and this allows the right estimation of the vessel length. However, it should be underlined that, when scatterers appears with such low RCS, sometimes they could be confused with some artefacts or multipath effects. In this case, the use of a sequence of ISAR images is important in order to discriminate between target scatterers and artefacts or multipath effects.

By comparing the ISAR image in the range/Doppler domain and the range/cross-range domain in Figure 6, 7 and 8, one can note that the target occupies different range cells. This is due to the cross-range scaling algorithm. Such algorithm takes as input the ISAR image in the range/Doppler domain and estimates the modulus of the target effective rotation vector in order to scale the Doppler axis from Hz to m. To estimate such scaling factor, the algorithm applies circular shifts to the original image. Such circular shifts are automatically estimated by the algorithm itself and may change among different ISAR image. The circular shifts are meant to shift each scatterer of the target in the centre of the ISAR image so as to effectively estimates its chirp rate which is in turn use to estimate the modulus of the target effective rotation vector. More details of such algorithm can be found in [28].

ISAR images however are used to estimate the target size and not the absolute range position of the scatterers with respect to the radar, which is instead may be given by the RD map. Then, whether the ISAR image in the range/cross-range domain appears shifted with respect to the ISAR image in the range/Doppler domain does not matter since this effects does not affect the estimation of the target size.

## DISCUSSIONS

In this work, we have investigated and demonstrated the ability of passive radar to detect, track and form a radar image of marine vessels (boats) in the proximity of harbours. The paper has reported results obtained with a technological demonstrator realized during a research program, named SMARP, founded by the Italian MoD and tested in several trials campaign in the area of the Livorno harbour (Italy), where the demonstrator is permanently installed. Livorno has been chosen as it represents a busy maritime hub, which is a significant scenario representative of several potential use cases. The ongoing research activities and expected future upgrades of the system are:

- RF front-end update to make it able to gather a larger bandwidth signal. In its current version the system is able to acquire a signal with an instantaneous bandwidth up to 25 MHz. However, it should be noted that a larger signal bandwidth is not guaranteed since the UHF spectrum is not generally completely filled by broadcast channels. Then, even if a larger bandwidth is acquired, spectral gaps may be present. This case has been recently addressed in literature and solved by using non-standard image formation techniques, such as Compressive Sensing (CS) based ISAR algorithms.
- The use of a dedicated IO transmitting a wideband noise-like and low power signal. According to international regulations, there are some bands that could be used for such purpose, namely, the Industrial, scientific and medical (ISM) radio bands. Among all the possible frequency ranges, the one between 2.4 GHz and 2.5 GHz has been identified as it offers a quite large bandwidth, a quite high operative frequency and is compatible with the current SMARP receivers.
- The SMARP system offers the possibility of simultaneously acquiring the signal in two polarization channels (H/V). Then, in the case of deploying a dedicated IO transmitting both H and V polarizations, the SMARP system would be able to acquire fully polarimetric data.

## CONCLUSIONS

The present work has been focused on the effectiveness of using passive radars with imaging capability for monitoring marine traffic. First of all, the "Software-defined multiband array passive radar (SMARP)" designed for maritime surveillance applications has been presented. The results obtained in a maritime scenario have demonstrated the capability of the system to detect and to track targets in UHF and S band respectively. The ISAR capability may be activated on a specific target of interest or may be performed simultaneously on all the detected targets. The results obtained on three different targets have proven that the system is able to estimate their

actual length. In view of all this, SMARP represents a potential system to improve the marine traffic monitoring and to support the formation of a common operational picture in harbor areas.

## ACKNOWLEDGMENT

The authors would like to thank the Centro di Supporto e Sperimentazione Navale - Istituto per le Telecomunicazioni e l'Elettronica "Giancarlo Vallauri" (CSSN-ITE), an experimental facility of the Italian Navy, for technical and logistic support given during the experiment that took place in Livorno. A special acknowledgement goes to the "V Reparto" of Segredifesa, which is the department of the Italian MoD in charge of the Technological Innovation, for funding the SMARP project, together with CNIT, within the contract number 20008.

## REFERENCES

[1] A. Weintrit, International Recent Issues about ECDIS, e-Navigation and Safety at Sea: Marine Navigation and Safety of Sea Transportation, CRC Press, 2011

[2] Di Lallo, A.; Farina, A.; Fulcoli, R.; Genovesi, P.; Lalli, R.; Mancinelli, R., "Design, development and test on real data of an FM based prototypical passive radar," in Radar Conference, 2008. RADAR '08. IEEE , vol., no., pp.1-6, 26-30 May 2008

[3] J. Palmer, D. Merrett, S. Palumbo, J. Piyaratna, S. Capon and H. Hansen, "Illuminator of Opportunity Bistatic Radar research at DSTO," 2008 International Conference on Radar, Adelaide, SA, 2008, pp. 701-705.

[4] P.E. Howland, D. Maksimiuk, G. Reitsma, FM radio based bistatic radar, Radar, Sonar and Navigation, IEE Proceedings, vol.152, no.3, pp. 107- 115, 3 June 2005

[5] Malanowski, M.; Kulpa, K.; Kulpa, J.; Samczynski, P.; Misiurewicz, J., "Analysis of detection range of FM-based passive radar," in Radar, Sonar & Navigation, IET , vol.8, no.2, pp.153-159, February 2014

[6] M. Glende , J. Heckenbach, H. Kuschel , S. Müller, J. Schell , C. Schumacher, Experimental passive radar systems using digital illuminators (DAB/DVB-T) International Radar Symposium (IRS) 2007 Cologne, Germany, 2007

[7] R. Zemmari, U. Nickel and W. D. Wirth, "GSM passive radar for medium range surveillance," Radar Conference, 2009. EuRAD 2009. European, Rome, 2009, pp. 49-52.

[8] R. Plšek, V. Stejskal, M. Pelant and M. Vojáček, "FM based passive coherent radar: From detections to tracks," Digital Communications - Enhanced Surveillance of Aircraft and Vehicles (TIWDC/ESAV), 2011 Tyrrhenian International Workshop on, Capri, 2011, pp. 123-127.

[9] H. D. Griffiths, C. J. Baker, "Passive coherent location radar systems. Part 1: Performance prediction," IEE Proc. Radar, Sonar and Navigation, vol. 152, no. 3, pp.153-159, June 2005.

[10] J. Raout, Sea target detection using passive DVB-T based radar, International Radar Conference 2008, Adelaide, Australia, 2-5 Sept. 2008

[11] K. Jamil, M. Alam, M. A. Hadi and Z. O. Alhekail, "A multi-band multi-beam software-defined passive radar part I: System design," Radar Systems (Radar 2012), IET International Conference on, Glasgow, UK, 2012, pp. 1-4.

[12] Edrich, M.; Schroeder, A., "Multiband multistatic Passive Radar system for airspace surveillance: A step towards mature PCL implementations," in Radar (Radar), 2013 International Conference on , vol., no., pp.218-223, 9-12 Sept. 2013

[13] F. Colone, P. Falcone, A. Macera and P. Lombardo, "High resolution cross-range profiling with Passive Radar via ISAR processing," 2011 12th International Radar Symposium (IRS), Leipzig, 2011, pp. 301-306

[14] P. Samczynski, K. Kulpa, M. K. Baczyk and D. Gromek, "SAR/ISAR imaging in passive radars," 2016 IEEE Radar Conference (RadarConf), Philadelphia, PA, 2016, pp. 1-6

[15] J. L. Garry, G. E. Smith and C. J. Baker, "Wideband DTV passive ISAR system design," 2015 IEEE Radar Conference (RadarCon), Arlington, VA, 2015, pp. 0834-0839

[16] Capria, A.; Petri, D.; Moscardini, C.; Conti, M.; Forti, A.C.; Massini, R.; Cerretelli, M.; Ledda, S.; Tesi, V.; Dalle Mese, E.; Gentili, G.B.; Berizzi, F.; Martorella, M.; Soleti, R.; Martini, T.; Manco, A., "Software-defined Multiband Array Passive Radar (SMARP) demonstrator: A test and evaluation perspective," in OCEANS 2015 – Genoa, vol., no., pp.1-6, 18-21 May 2015

[17] M. Conti, C. Moscardini and A. Capria, "Dual-polarization DVB-T passive radar: Experimental results," 2016 IEEE Radar Conference (RadarConf), Philadelphia, PA, 2016, pp. 1-5.

[18] J. E. Palmer, H. A. Harms, S. J. Searle and L. Davis, "DVB-T Passive Radar Signal Processing," in IEEE Transactions on Signal Processing, vol. 61, no. 8, pp. 2116-2126, April15, 2013.

[19] J.E. Palmer, S.J. Searle, "Evaluation of adaptive filter algorithms for clutter cancellation in Passive Bistatic Radar," Radar Conference (RADAR), 2012 IEEE , pp.493-498, 7-11 May 2012.

[20] Moscardini, C.; Petri, D.; Capria, A.; Conti, M.; Martorella, M.; Berizzi, F., "Batches algorithm for passive radar: a theoretical analysis," in Aerospace and Electronic Systems, IEEE Transactions on , vol.51, no.2, pp.1475-1487, April 2015

[21] C. R. Berger, B. Demissie, J. Heckenbach, P. Willett, "Signal Processing for Passive Radar Using OFDM Waveforms," Selected Topics in Signal Processing, IEEE Journal of , vol.4, no.1, pp.226,238, Feb. 2010.

[22] C. Moscardini, M. Conti, F. Berizzi, M. Martorella, A. Capria, "Spatial Adaptive Processing for Passive Bistatic Radar," Radar Conference, 2014 IEEE , vol., no., pp.1061,1066, 19-23 May 2014.

[23] D. Pasculli, A. Baruzzi, C. Moscardini, D. Petri, M. Conti, M. Martorella, "DVB-T Passive Radar Tracking on Real Data Using Extended Kalman Filter with DOA Estimation," in Proc. at the International Radar Symposium (IRS-2013), Dresden, Germany, June 19-21,2013.

[24] M. Conti, F. Berizzi, M. Martorella, E. D. Mese, D. Petri and A. Capria, "High range resolution multichannel DVB-T passive radar," in IEEE Aerospace and Electronic Systems Magazine, vol. 27, no. 10, pp. 37-42, Oct. 2012.

[25] Wei Qiu; Giusti, E.; Bacci, A.; Martorella, M.; Berizzi, F.; Hongzhong Zhao; Qiang Fu, "Compressive sensing based algorithm for passive bistatic ISAR with DVB-T signals," in Aerospace and Electronic Systems, IEEE Transactions on , vol.51, no.3, pp.2166-2180, July 2015

[26] Martorella, M.; Giusti, E., "Theoretical foundation of passive bistatic ISAR imaging," in Aerospace and Electronic Systems, IEEE Transactions on , vol.50, no.3, pp.1647-1659, July 2014

[27] Olivadese, D.; Giusti, E.; Petri, D.; Martorella, M.; Capria, A.; Berizzi, F., "Passive ISAR With DVB-T Signals," in Geoscience and Remote Sensing, IEEE Transactions on , vol.51, no.8, pp.4508-4517, Aug. 2013

[28] M. Martorella, "Novel approach for ISAR image cross-range scaling," in IEEE Transactions on Aerospace and Electronic Systems, vol. 44, no. 1, pp. 281-294, January 2008